

# Compact Tunable Bandpass Filter with Continuous Control of Center Frequency and Bandwidth Independently

Liangzu Cao\* and Lixia Yin

*School of Mechanical and Electronic Engineering of Jingdezhen Ceramic University, Jingdezhen, China*

**ABSTRACT:** This paper presents a compact electrically tunable bandpass filter with continuous control of center frequency and bandwidth independently. The filter consists of two coaxial dielectric resonators loaded with two varactors for center frequency tuning. A symmetrical Y-type capacitor network used for tuning bandwidth is proposed. A prototype made of dielectric ceramics with dielectric constant of 88 has been designed, fabricated, and measured. The center frequency varies from 0.562 GHz to 0.845 GHz, and 3 dB bandwidth is tuned from 117 MHz to 194 MHz at the center frequency of 845 MHz. A constant absolute bandwidth of 141 MHz is realized by varying simultaneously bias voltages. The volume of fabricated filter containing bias networks is  $24 \times 22 \times 6.5 \text{ mm}^3$  ( $0.045\lambda_0 \times 0.041\lambda_0 \times 0.012\lambda_0$ ). The measured results agree with the simulation outcome.

## 1. INTRODUCTION

Reconfigurable or tunable filters are highly demanded in modern wireless communication systems and have attracted great attention due to their potential for size and complexity reduction [1]. Center frequency and bandwidth tunable filters are especially useful for the design of high-frequency multifunction receivers that simultaneously support multiple information signals with different frequency bands and power-level characteristics. These filters are capable of eliminating out-of-band noises, jamming spectral components, and preserving the dynamic range under any signal-receiving conditions [2]. The technology of center frequency tunable filters is quite mature, while bandwidth tuning or controlling is more challenging than frequency tuning [3]. There are two kinds of bandpass filters (BPFs) with tunable bandwidths: discrete tunable bandwidth filters and continuously tunable bandwidth filters. PIN switches and micro electromechanical systems (MEMSs) are employed to accomplish discrete bandwidth tunable filters [4–9]. Varactors are used to continuously tune bandwidths besides the center frequency of BPFs [1, 10–20]. Mao et al. [10] and Chen and Yang [1] utilized a tri-mode cross-shaped resonator (TCSR) and two TCSRs to realize a bandwidth and center frequency tunable BPF, respectively, but the use of many varactors resulted in high costs. Chao et al. [11] proposed a H-type multi-mode resonator (MMR) loaded with varactors to realize a reconfigurable BPF with separately relocatable passband edge. Chaudhary et al. [12] controlled even-mode resonant frequencies independently to tune the bandwidth while keeping odd-mode resonant frequencies constant. Huang et al. [13] proposed a quadruple-mode resonator BPF with tunable bandwidth by varying the high-side edge and low-side edge of the passband. Jia et al. [14] proposed a tri-mode resonator BPF with bandwidth reconfigurable by

adjusting each passband edge of the filter. Tsai et al. [15] proposed a loop-shaped dual-mode resonator that is perturbed with three varactors to realize center frequency tunability and passband configurability. There are also some methods based on single mode resonators [2, 16–20]. Sánchez-Renedo et al. [2] placed variable coupling reducers between resonators to tune bandwidth, but the resonance peaks appear near the filter passband. Wei et al. [16] and Fan et al. [17] cascaded a tunable low-pass unit together with a tunable high-pass unit to form a bandpass filter with a reconfigurable center frequency and bandwidth independently by tuning the frequencies of the band edges, but the designs are complicated. Chiou and Rebeiz [18], Schuster et al. [19], and Tang and Hong [20] inserted varactors between two resonators to tune the bandwidth; however, the position connected a varactor has a significant effect on the tuning performance.

The tunable filters mentioned above adopted microstrip structures and were fabricated on a substrate with low dielectric constant ( $\epsilon_r \leq 10$ ), large size, and high insertion loss while coaxial dielectric resonators (CDRs) made of high dielectric constant ( $\epsilon_r \geq 20$ ) ceramics have the advantages of small volume, high quality factor, and good temperature stability. However, tunable coaxial dielectric filters are rarely reported in the literature. Wang et al. [21] designed a second-order tunable coaxial dielectric filter, but the design is complicated and expensive. The authors in [22, 23] have developed tunable BPFs with constant bandwidth, but their bandwidths are not tunable. References [24, 25] designed tunable dielectric filters, but their structures are not coaxial dielectric filters, so their volumes are large.

In this paper, a compact tunable dielectric BPF with continuous independent control of center frequency and bandwidth is proposed. A symmetrical Y-type capacitor network is located between two CDRs to continuously tune the bandwidth (BW).

\* Corresponding authors: Liangzu Cao (clz4233@aliyun.com).

Two varactors are loaded at the open ends of CDRs for center frequency tuning.

## 2. DESIGN PROCEDURE

Figure 1 shows the structure of the proposed tunable bandpass filter. It is composed of a pair of CDRs loaded with varactors (MA46H206). The CDRs were made of microwave ceramics with  $\varepsilon_r$  of 88. Its physical dimensions are 1.5 mm inner diameter, 6 mm side length, and 7 mm height. A varactor (SMV1413-079LF, denoted by  $C_{cr}$ ) and two fixed capacitors (denoted by  $C_{1A}$ ) form a Y-type capacitor network between CDRs. Lumped capacitors (denoted by  $C_{01}$  and  $C_{23}$ ) are used for coupling to the I/O ports. Three resistors (denoted by  $R_b$ ) are used for DC bias to reduce the RF-signal leakage through the bias networks. Two fixed capacitors (denoted by  $C_B$ ) are connected in series with varactors to block DC.

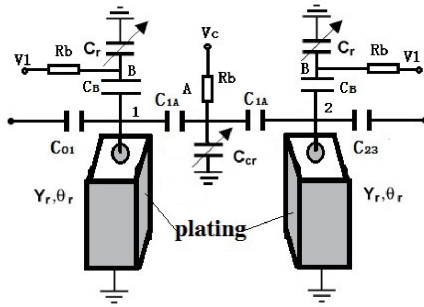


FIGURE 1. Structure of the proposed tunable bandpass filter.

### 2.1. Structure and Characteristic of Coaxial Dielectric Resonator

The coaxial dielectric resonator is a hollow tube filled with microwave dielectric ceramics. The surfaces of the resonator are covered by silver layers except one end. Figure 2 shows the structure of a coaxial dielectric resonator.

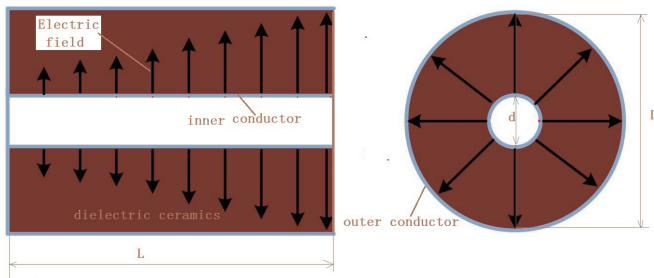


FIGURE 2. Structure of a coaxial dielectric resonator.

The main performances of the resonator are the resonant frequency, characteristic impedance or characteristic admittance, and unloaded quality factor ( $Q_u$ ). The manufacture process of a resonator needs to go through a series of processes to complete, such as powder preparation, dry pressing, sintering, and surface metallization. The resonator is connected to an external circuit by a metal tab. Just like the metal cavity model, the simulation model of the coaxial dielectric resonator can be built by filling the metal cavity with dielectric material.

The resonant frequency of a single resonator can be estimated by the following formula [26],

$$Y_{in} = j\omega \frac{C_r C_b}{C_r + C_b} - jY_r \cot \theta_r = 0 \quad (1)$$

where  $Y_r$  and  $\theta_r$  are characteristic admittance and electrical length of the resonator, and they can be expressed as [26],

$$Y_r = \frac{\sqrt{\varepsilon_r}}{60 \cdot \ln(D/d)} \quad (2)$$

$$\theta_r = \omega \cdot l \cdot \sqrt{\varepsilon_r} / c \quad (3)$$

where  $\varepsilon_r$ ,  $D$ ,  $d$ , and  $l$  are relative dielectric constant, outer diameter, inner diameter, and length of a dielectric coaxial resonator, respectively, and  $c$  is the velocity of light.

Unloaded quality factor ( $Q_u$ ) is frequently used in discussing the “Figure of merit” of a resonator. In broad terms,  $Q_u$  is a significant parameter applied in circuit design for the evaluation of electrical performance and is generally obtained by numerical analysis using high-speed computers. In the case of a coaxial resonator, closed form equations for unloaded- $Q$  can be derived by analytical methods [26].

$$\frac{1}{Q_u} = \frac{1}{Q_c} + \frac{1}{Q_d} = \frac{1}{Q_c} + \tan \delta_d \quad (4)$$

where  $Q_c$  is determined by the side-wall conductor loss of the resonator;  $Q_d$  is quality factor of the dielectric ceramics;  $\tan \delta_d$  represents dielectric loss.

$$Q_c = \frac{D}{\delta} \cdot \frac{\pi \ln(D/d)}{\pi(1 + D/d) + (D/l) \cdot \ln(D/d)} \quad (5)$$

where  $\delta$  is the skin depth,  $\delta = 1/\sqrt{\pi \cdot f \cdot \mu_0 \cdot \sigma}$ , and  $\sigma$  is the conductivity of the conductor.

The resonator in this work is made of BaO-TiO<sub>2</sub>-Nd<sub>2</sub>O<sub>3</sub> ceramics with  $Q_u$  more than 300.

### 2.2. Design Parameters

We employed high frequency structure simulator (HFSS) to extract the coupling coefficient  $k$  and the quality factor  $Q_e$ . These parameters can be calculated using Eqs. (6) and (7) [27].

$$k = \frac{f_2^2 - f_1^2}{f_2^2 + f_1^2} \quad (6)$$

$$Q_e = \frac{f_0}{BW_{3dB}} \quad (7)$$

where  $f_2$  and  $f_1$  are the higher and lower resonant frequencies of coupled resonators, and  $f_0$  and  $BW_{3dB}$  represent the center frequency and 3 dB bandwidth of the resonance curve, respectively.

Figure 3 presents the variation of coupling coefficient and center frequency with capacitance of variable  $C_{cr}$ . It is found that coupling coefficient is inversely proportional to capacitance. This is due to the conversion of Y-type capacitor network into  $\Delta$ -type one, as shown in Figure 4.

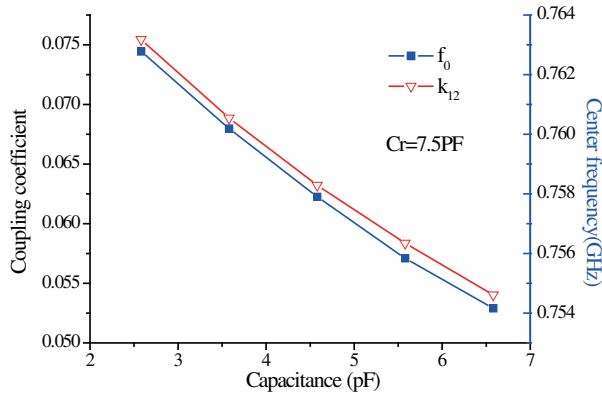


**FIGURE 3.** Variation of coupling coefficient and center frequency with capacitance of variable  $C_{cr}$ .

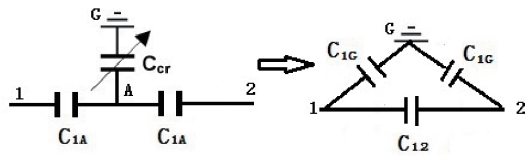


**FIGURE 4.** Conversion of Y-type capacitor network into  $\Delta$ -type one.

In Figure 4,  $C_{12}$  is a coupling capacitor between two DRs, and  $C_{1G}$  is the shunt capacitance loaded with the open end of DR.  $C_{12}$  can be calculated by the following equations,

$$C_{12} = \frac{C_{1A}^2}{2C_{1A} + C_{cr}} \quad (8)$$

Figure 5 shows coupling coefficient and external quality factor ( $Q_e$ ) as a function of tuning frequency. With the increase of frequency, the coupling coefficient increases, and  $Q_e$  value decreases. These relationships meet the requirements of a band-pass filter.

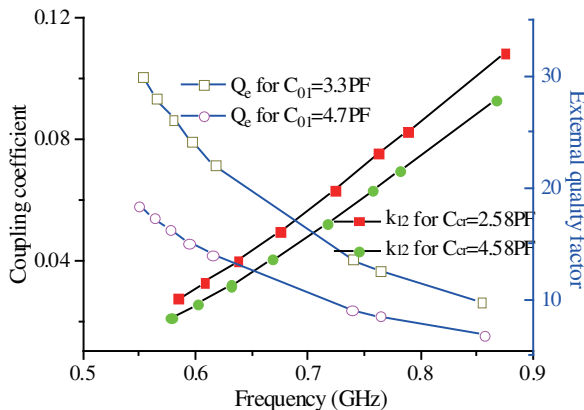


**FIGURE 5.** Variation of coupling coefficient and External quality factor with tuning frequency.

### 2.3. Design of the Filter with Tunable Center Frequency

The capacitance ratios of the varactors for the center frequency tuning are determined according to the design method [3, 28].

Based on HFSS simulation, the design parameters are as follows:  $C_{01}$  is equal to 3.3 pF (0603, ATC);  $C_{cr}$  ranges from 2.58 pF to 6.58 pF; and  $C_r$  ranges from 21.5 pF to 3.5 pF. When the loaded capacitance changes from 21.5 pF to 3.5 pF, the central frequency varies from 0.56 GHz to 0.84 GHz, and the 3 dB bandwidth changes from 24 MHz to 136 MHz. Figure 6 shows the simulated results.

## 3. EXPERIMENTAL RESULTS AND DISCUSSION

The filter was fabricated on a Rogers RT/duroid 5880 substrate with a dielectric constant of 2.2 and thickness of 0.5 mm, and measured using a network analyzer E5701B.

### 3.1. Measurement of the Filter with Tunable Center Frequency

The measured performance of the proposed filter is presented in Figure 6, where the tuning frequency varies from 0.562 GHz to 0.845 GHz when bias voltages applied to MA46H206 varactors change from 3.5 V to 20 V, while the bias voltage applied to SMV1413 varactor is fixed at 10 V. The tuning range is a little different from the simulated result because the simulation neglects the parasitic parameters of chip components, and the fabrication technology produces tolerances.

The 3 dB bandwidth and insertion loss of the fabricated filter are listed as follows: the bandwidth changes from 36 MHz to 194 MHz, and the insertion loss varies from 4.4 dB to 0.6 dB. It is observed that the measured values of 3 dB bandwidth and insertion loss are different from the simulated values. The larger measured insertion loss at 0.562 GHz and 0.60 GHz is due to the low Q value ( $< 100$ ) of the varactors and smaller fractional bandwidth (6.4%) at these frequencies. The difference between the measured and simulated values of 3 dB bandwidth is attributed to the parasitic parameters of chip components (fixed capacitors and varactors).

### 3.2. Measurement of the Filter with Tunable Bandwidth

When the bias voltage applied to MA46H206 varactors is fixed at 20 V and that applied to SMV1413 varactor varies between 1 V and 10 V, the performance of this filter was measured, as shown in Figure 7. It is observed that the bandwidth tuning ranges from 117 MHz to 194 MHz, but the reflection loss becomes worse with the decrease of the bias voltage due to the constant external quality factor during tuning. The center frequency is found to shift right because odd-mode frequency rises, while even-mode frequency keeps constant during tuning.

The mechanism of bandwidth tuning is that the inter-stage coupling increases with the increase of the bias voltage of SMV1413, and the higher the bias voltage is, the larger the coupling coefficient is. This phenomenon is produced by the Y-type capacitor network for coupling. It is well known that the capacitance of a varactor is inversely proportional to the bias voltage, and the inter-stage coupling coefficient is inversely proportional to the capacitance of a varactor (seeing Figure 2); therefore, the inter-stage coupling coefficient is proportional to the bias voltage, corresponding to the case of Figure 7.

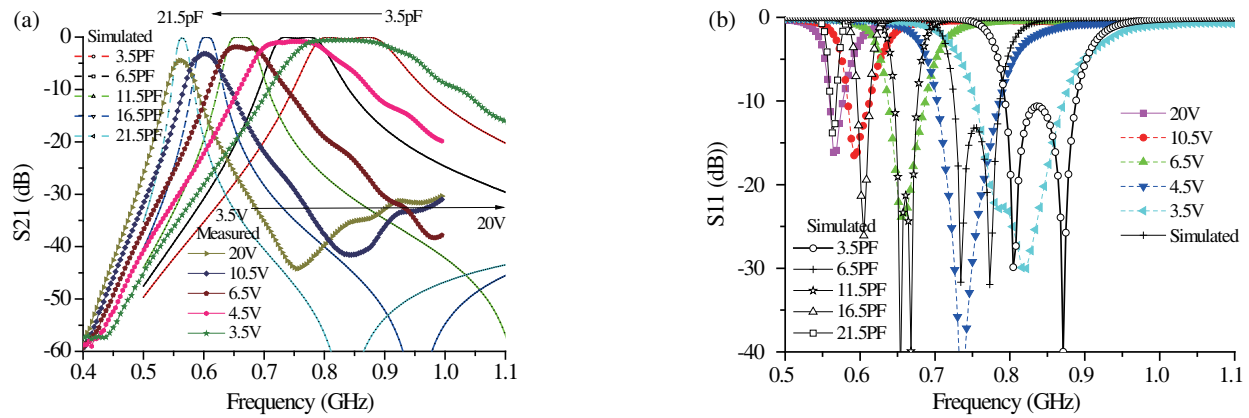


**FIGURE 6.** Measured and simulated responses of the proposed filter. (a) Transmission response. (b) Reflection response.

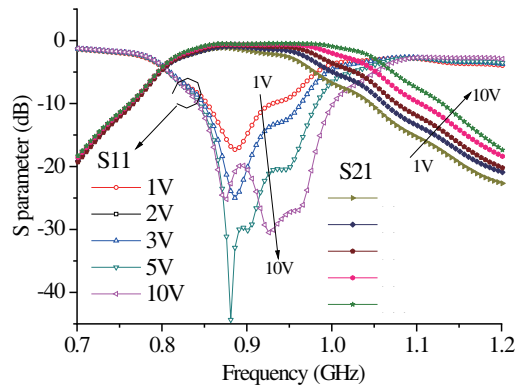


**FIGURE 7.** Measured responses of the proposed filter with tunable bandwidth.

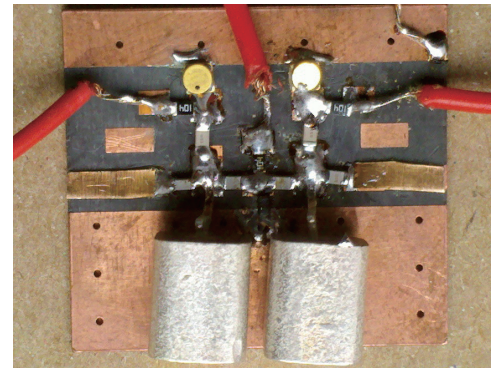


**FIGURE 8.** Photo of the proposed filter.

**TABLE 1.** Performance comparison among tunable filters.

	Frequency Tuning (GHz)	BW Tuning (MHz) or FBW	Coupling structure	Area (mm <sup>2</sup> )
[2]	0.47–0.86	~ 16–18.5 (at 850 MHz)	detuned resonator	50 × 65 (0.078λ <sub>0</sub> × 0.10λ <sub>0</sub> )
[12]	1.48 to 1.8	5.76%–8.55%	dual-Mode and a varactor	~ 25 × 50 (0.12λ <sub>0</sub> × 0.25λ <sub>0</sub> )
	2.40–2.88	8.28%–12.42%		
[13]	Fixed at 2	440–680	quadruple-mode and varactors	~ 25 × 50 (0.17λ <sub>0</sub> × 0.33λ <sub>0</sub> )
[15]	0.43–0.6	16–55 (at 600 MHz)	dual-Mode and varactors	30 × 40 (0.05λ <sub>0</sub> × 0.057λ <sub>0</sub> )
[18]	1.5–2.2	50–170	high-impedance lines and varactors	~ 35 × 50 ((0.175λ <sub>0</sub> × 0.25λ <sub>0</sub> )
[21]	0.8–1.1	6 ~ 13%	RF-MEMS digital capacitors	~ 23 × 25 (0.061λ <sub>0</sub> × 0.067λ <sub>0</sub> )
[24]	4.87–4.97	no	coupling iris	250 × 450 (4.0λ <sub>0</sub> × 7.3λ <sub>0</sub> )
[25]	15.62–15.86	no	coupling iris	~ 15 × 20 (0.78λ <sub>0</sub> × 1.0λ <sub>0</sub> )
This work	0.562–0.845	117–194 (at 845 MHz)	Y-type capacitor network	24 × 22 (0.045λ <sub>0</sub> × 0.041λ <sub>0</sub> )

Figure 8 shows a photo of proposed tunable filter. The volume of filter containing bias networks is  $24 \times 22 \times 6.5 \text{ mm}^3$  ( $0.045\lambda_0 \times 0.041\lambda_0 \times 0.012\lambda_0$ ), where  $\lambda_0$  corresponds to the wavelength of the center frequency of 0.562 GHz in free space.

### 3.3. Measurement of the Filter with Constant Absolute Bandwidth

Figure 9 shows the measured results of this filter with constant absolute bandwidth of 141 MHz, and the inset also presents the wideband performance of the filter.

The reason that the absolute bandwidth of the filter is kept constant during the center frequency tuning is that the inter-stage coupling is inversely proportional to the tuning frequency, while the external quality is proportional to the tuning frequency [23]. As can be seen in Figure 6, the 3 dB bandwidth ( $\text{bw}_{3\text{dB}}$ ) of the filter increases with the increase of the bias voltage ( $V_c$ ) when the center frequency of the filter is not tuned, while the center frequency ( $f_0$ ) of the filter decreases with the increase of the bias voltage ( $V_1$ ), therefore, when  $V_1$  is smaller,  $V_c$  larger,  $f_0$  lower, and  $\text{bw}_{3\text{dB}}$  becomes larger. It meets the



condition that the bandwidth is constant when the center frequency is tuned, corresponding to the case of Figure 8.

Table 1 describes the performance comparison between the proposed work and the literature, which shows that the filter has the advantages of small volume and novel coupling structure.

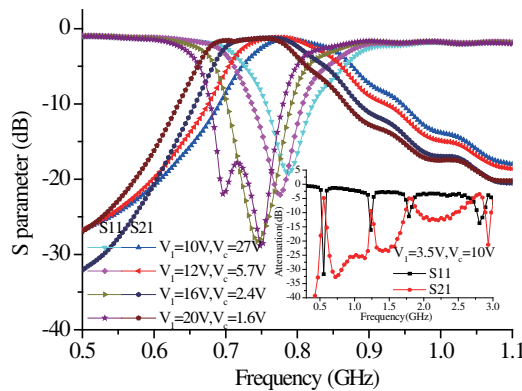


**FIGURE 9.** Measured responses of this filter with constant absolute bandwidth and wide band performance.

#### 4. CONCLUSION

A tunable bandpass filter with tunable center frequency and bandwidth has been designed and fabricated. A Y-type capacitor network with a varactor was used to couple resonators to tune the bandwidth. This structure can efficiently reduce the size and complexity of the filter. The proposed filter can flexibly realize various center frequencies and bandwidths by replacing dielectric resonators and varactors. For example, dielectric resonators with dielectric constant of 38 or 20 can be used to design 1.5 GHz GPS tunable filters or 2.4 GHz Wi-Fi tunable filters. Other variable elements such as MA46H204 can be used for coupling to extend the bandwidth tuning range. It is expected that the proposed tunable filter structure could be used for more than two-poles filters and VHF/UHF filters in multi-band communication systems.

#### ACKNOWLEDGEMENT

This work was supported in part by the National Natural Science Foundation of China [grant number: 61661023]; PhD research startup foundation of Jingdezhen Ceramic University of China [grant number: 2018-01]; Educational Commission of Jiangxi Province of China [No. GJJ201305].

#### REFERENCES

- [1] Chen, A. and T. Yang, "A microstrip bandpass filter with tunable bandwidth and center frequency," *Microwave and Optical Technology Letters*, 1–4, 2021.
- [2] Sánchez-Renedo, M., R. Gómez-García, J. I., and C. Briso-Rodríguez, "Tunable combine filter with continuous control of center frequency and bandwidth," *IEEE Transactions on Microwave Theory and Techniques*, Vol. 53, No. 1, 191–199, Jan. 2005.
- [3] Hong, J.-S. and C. Briso-Rodríguez, *Tunable and Reconfigurable Filters*, in *Microstrip Filters for RF Microwave Applications*, 564–569, John Wiley & Sons, Inc., 2011.
- [4] Bandyopadhyay, A., P. Sarkar, and R. Ghatak, "A bandwidth reconfigurable bandpass filter for ultrawideband and wideband applications," *IEEE Transactions on Circuits and Systems II-express Briefs*, Vol. 69, No. 6, 2747–2751, Jun. 2022.
- [5] Arain, S., A. Quddious, S. Nikolaou, and P. Vryonides, "Demonstration of reconfigurable BPFs with wide tuning bandwidth range using  $3\lambda/4$  open- and  $\lambda/2$  short-ended stubs," *Technologies*, Vol. 8, No. 14, 1–12, Mar. 2020.
- [6] Kawai, K., H. Okazaki, and S. Narahashi, "Center frequency and bandwidth independently tunable filter using MEMS digitally tunable capacitors," in *2014 Xxxith URSI General Assembly and Scientific Symposium (URSI GASS)*, 29th URSI General Assembly and Scientific Symposium (URSI GASS), Beijing, China, Aug. 16–23, 2014.
- [7] Sanchez-Soriano, M., R. Gomez-Garcia, G. Torregrosa-Penalva, and E. Bronchalo, "Reconfigurable-bandwidth bandpass filter within 10–50%," *IET Microwaves Antennas & Propagation*, Vol. 7, No. 7, 502–509, May 15, 2013.
- [8] Liu, B., F. Wei, H. Zhang, X. Shi, and H. Lin, "A tunable bandpass filter with switchable bandwidth," *Journal of Electromagnetic Waves and Applications*, Vol. 25, No. 2–3, 223–232, 2011.
- [9] Gentili, F., L. Pelliccia, F. Cacciamani, P. Farinelli, and R. Sorrentino, "RF MEMS bandwidth-reconfigurable hairpin filters," in *2012 Asia-Pacific Microwave Conference (APMC 2012)*, 735–737, Kaohsiung, Taiwan, Dec. 04–07, 2012.
- [10] Mao, J.-R., W.-W. Choi, K.-W. Tam, W. Che, and Q. Xue, "Tunable bandpass filter design based on external quality factor tuning and multiple mode resonators for wideband applications," *IEEE Transactions on Microwave Theory and Techniques*, Vol. 61, No. 7, 2574–2584, Jul. 2013.
- [11] Chao, S.-F., W.-C. Lin, and C.-Y. Kuo, "Bandpass filter with tunable bandwidth using triple-mode H-type resonator," in *2014 International Symposium on Next-generation Electronics (ISNE)*, 3rd International Symposium on Next-generation Electronics (ISNE), Chang Gung Univ, Taoyuan, Taiwan, May 07–10, 2014.
- [12] Chaudhary, G., Y. Jeong, and J. Lim, "Dual-band bandpass filter with independently tunable center frequencies and bandwidths," *IEEE Transactions on Microwave Theory and Techniques*, Vol. 61, No. 1, 1, 107–116, Jan. 2013.
- [13] Huang, X., Q. Feng, and Q. Xiang, "Bandpass filter with tunable bandwidth using quadruple-mode stub-loaded resonator," *IEEE Microwave and Wireless Components Letters*, Vol. 22, No. 4, 176–178, Apr. 2012.
- [14] Jia, D., Q. Feng, X. Huang, and Q. Xiang, "A novel tri-mode bandwidth tunable filter with harmonic suppression," *Progress In Electromagnetics Research C*, Vol. 34, 183–194, 2013.
- [15] Tsai, H.-J., N.-W. Chen, and S.-K. Jeng, "Center frequency and bandwidth controllable microstrip bandpass filter design using loop-shaped dual-mode resonator," *IEEE Transactions on Microwave Theory and Techniques*, Vol. 61, No. 10, 3590–3600, Oct. 2013.
- [16] Wei, Z., T. Yang, P.-L. Chi, X. Zhang, and R. Xu, "A 10.23–15.7-GHz varactor-tuned microstrip bandpass filter with highly flexible reconfigurability," *IEEE Transactions on Microwave Theory and Techniques*, Vol. 69, No. 10, 4499–4509, Oct. 2021.
- [17] Fan, M., K. Song, and Y. Fan, "Reconfigurable bandpass filter with wide-range bandwidth and frequency control," *IEEE Transactions on Circuits and Systems II-express Briefs*, Vol. 68, No. 6, 1758–1762, Jun. 2021.
- [18] Chiou, Y.-C. and G. Rebeiz, "Tunable 1.55–2.1 GHz 4-pole elliptic bandpass filter with bandwidth control and > 50 dB rejection for wireless systems," *IEEE Transactions on Microwave Theory and Techniques*, Vol. 61, No. 1, 1, 117–124, Jan. 2013.

- [19] Schuster, C., A. Wiens, F. Schmidt, M. Nickel, M. Schuessler, R. Jakoby, and H. Maune, "Performance analysis of reconfigurable bandpass filters with continuously tunable center frequency and bandwidth," *IEEE Transactions on Microwave Theory and Techniques*, Vol. 65, No. 11, 2, SI, 4572–4583, Nov. 2017.
- [20] Tang, W. and J. Hong, "Reconfigurable microstrip combline filter with tunable center frequency and bandwidth," in *Asia-Pacific Microwave Conference 2011*, 1162–1165, Engineers Australia, Melbourne, Australia, Dec 05–08, 2011.
- [21] Wang, H., A. Anand, and X. Liu, "A miniature 800–1100-MHz tunable filter with high-Q ceramic coaxial resonators and commercial RF-MEMS tunable digital capacitors," in *2017 IEEE 18th Wireless and Microwave Technology Conference (WAMTCON)*, 1–3, Cocoa Beach, FL, Apr. 24–25, 2017.
- [22] Cao, L., G. Li, J. Hu, and L. Yin, "A miniaturized tunable bandpass filter with constant fractional bandwidth," *Progress in Electromagnetics Research C*, Vol. 57, 89–97, 2015.
- [23] Cao, L., J. Yan, and L. Yin, "A compact tunable dielectric filter with constant absolute bandwidth," in *2018 International Conference on Microwave and Millimeter Wave Technology (ICMMT 2018)*, 1–3, Chengdu, China, May 06–09, 2018.
- [24] Huang, F., S. Fouladi, and R. Mansour, "High-Q tunable dielectric resonator filters using MEMS technology," *IEEE Transactions on Microwave Theory and Techniques*, Vol. 59, No. 12, 3401–3409, Dec. 2011.
- [25] Yan, W. and R. Mansour, "Tunable dielectric resonator bandpass filter with embedded MEMS tuning elements," *IEEE Trans. Microwave Theory and Tech.*, Vol. 55, No. 1, 154–160, Jan. 2007.
- [26] Pozar, D. and R. Mansour, *Microwave Engineering*. John Wiley & Sons, Inc., New Jersey, 2011.
- [27] Hong, J.-S. and R. Mansour, *Coupled Resonator Circuits, in Microstrip Filters for RF Microwave Applications*, 3rd ed., 244–262, John Wiley & Sons, Inc., New Jersey, 2011.
- [28] Torregrosa-Penalva, G., G. Lopez-Risueno, and J. Alonso, "A simple method to design wide-band electronically tunable combline filters," *IEEE Transactions on Microwave Theory and Techniques*, Vol. 50, No. 1, 172–177, 2002.